

1 **Supplementary Material for**

2

3 **Monitoring SARS-CoV-2 in wastewater during New York City's second wave of COVID-**
4 **19: Sewershed-level trends and relationships to publicly available clinical testing data**

5 Catherine Hoar,^a Francoise Chauvin,^b Alexander Clare,^b Hope McGibbon,^b Esmeraldo Castro,^b
6 Samantha Patinella,^b Dimitrios Katehis,^b John J. Dennehy,^{c,d} Monica Trujillo,^e Davida S.
7 Smyth,^{f,g} Andrea I. Silverman^{a*}

8

9 ^aDepartment of Civil and Urban Engineering, New York University Tandon School of
10 Engineering Brooklyn, NY, USA

11 ^bNew York City Department of Environmental Protection, New York, NY, USA

12 ^cBiology Department, Queens College, The City University of New York, Queens, NY USA

13 ^dBiology Doctoral Program, The Graduate Center, The City University of New York, New York,
14 NY, USA

15 ^eDepartment of Biology, Queensborough Community College, The City University of New
16 York, Bayside, NY, USA

17 ^fDepartment of Natural Sciences and Mathematics, Eugene Lang College of Liberal Arts at The
18 New School, New York, NY, USA

19 ^gpresent affiliation: Department of Life Sciences, Texas A&M University San Antonio, San
20 Antonio, Texas, USA

21

22 *corresponding author: Andrea Silverman, andrea.silverman@nyu.edu

23

24 **Table of Contents**

25 Table S.1. New York City’s 14 wastewater resource recovery facilities (WRRFs) S3

26 **Sample Processing and RNA Extraction Methodology** S4

27 **RT-qPCR Assays** S6

28 *SARS-CoV-2 N1 Assay* S6

29 Table S.2. MIQE checklist: Essential and desirable information for the SARS-CoV-2 N1 target
30 RT-qPCR assay⁷ S8

31	Figure S.1. SARS-CoV-2 viral loads in wastewater from the Wards Island facility calculated	
32	using (a) the individual standard curves associated with the RT-qPCR plate on which each	
33	sample was run and (b) the pooled standard curve.	S13
34	<i>BCoV Assay</i>	S13
35	Publicly Available Clinical COVID-19 Data and Hospitalization Data	S15
36	Figure S.2. Summary of COVID-19 testing data (molecular tests) for each sewershed in New	
37	York City.	S16
38	Figure S.3. Summary of 7-day averages of new cases (solid red line) and hospitalizations	
39	(dashed black line) normalized by borough population for each New York City borough for	
40	the study period.	S17
41	Sewershed-level Spearman's Rank Correlation Coefficients	S18
42	Table S.3. Spearman's rank correlation coefficients (ρ) between SARS-CoV-2 wastewater	
43	data and clinical COVID-19 case data for each sewershed in New York City.	S18
44	Time Lag Analysis	S19
45	Figure S.4. Spearman rank correlation coefficients (ρ) between SARS-CoV-2 viral loads (N1	
46	GC/day) and 7-day averages of new COVID-19 cases/day, with a time lag (τ) between 0 and	
47	21 days for each sewershed in New York City.	S20
48	Linear Regression Analysis	S21
49	Figure S.5. Linear regression of \log_{10} -transformed flow-normalized SARS-CoV-2 viral loads	
50	in wastewater (N1 GC/day) and \log_{10} -transformed 7-day averages of new COVID-19	
51	cases/day for the combined data set without the data filtered based on potentially inadequate	
52	testing.	S21
53	Estimation of Minimum Detectable Case Rates	S22
54	Table S.4. Estimated minimum detectable case rates (new COVID-19 cases/day/100,000)	
55	associated with method LOD for quantification of the SARS-CoV-2 N1 gene target in	
56	wastewater (4,500 N1 GC/L) for each sewershed.	S23
57	Figure S.6. Estimation of new COVID-19 cases/day associated with the method LOD for	
58	quantification of the SARS-CoV-2 N1 gene target in wastewater, based on the linear	
59	regression of \log_{10} -transformed SARS-CoV-2 viral loads (N1 GC/day) and \log_{10} -transformed	
60	7-day averages of new COVID-19 cases/day for the combined data set (modified from Figure	
61	3.a).	S24
62	References	S25
63		
64		
65		

66
67

Table S.1. New York City’s 14 wastewater resource recovery facilities (WRRFs)

Wastewater Resource Recovery Facility (WRRF)	Borough(s)	Population Served*	Daily Flow Range (Average)[†] in MGD
Hunts Point	Bronx	755,948	115 - 215 (136)
Wards Island	Bronx and Manhattan	1,201,485	143 - 273 (180)
North River	Manhattan	658,596	81 - 143 (94)
Newtown Creek	Manhattan and Brooklyn	1,156,473	158 - 296 (188)
Red Hook	Brooklyn	224,029	21 - 46 (26)
Owls Head	Brooklyn	906,442	81 - 159 (95)
Coney Island	Brooklyn	682,342	70 - 102 (82)
26th Ward	Brooklyn	290,608	44 - 89 (55)
Rockaway	Queens	120,539	18 - 25 (20)
Jamaica Bay	Queens	748,737	74 - 103 (81)
Tallman Island	Queens	449,907	48 - 90 (59)
Bowery Bay	Queens	924,695	82 - 179 (100)
Port Richmond	Staten Island	226,167	23 - 55 (29)
Oakwood Beach	Staten Island	258,731	24 - 41 (28)

68 *Based on inter-census population estimates for 2020 from the New York Metropolitan
69 Transportation Council’s 2050 Socioeconomic and Demographic Forecast¹

70 [†]Average (Q_{avg}) is based on daily flows from November 8, 2020 to April 11, 2021

71
72

73 **Sample Processing and RNA Extraction Methodology**

74 Influent wastewater samples were analyzed in 40-mL aliquots using polyethylene glycol (PEG)
75 precipitation for virus concentration. To ensure inactivation of viruses before sample
76 concentration, samples were first pasteurized at 60 °C in a water bath for a total of 90 min, which
77 allowed 30 min for the sample to reach 60 °C and then 60 min of incubation at that temperature.
78 Pasteurized samples were cooled in a room temperature water bath for 10 min followed by a 10
79 min incubation on ice prior to addition of an attenuated bovine coronavirus (BCoV) from a
80 bovine rota-coronavirus vaccine (Calf-Guard®; Zoetis #4002), which was used as a process
81 control. The BCoV control spike was prepared based on a method modified from Feng et al.,
82 2021.² One one-dose vial of the Calf-Guard® vaccine was rehydrated with 1 mL TE buffer
83 (Fisher Scientific, BP2473100) and stored in single-use aliquots at -80 °C. On the day of sample
84 analysis, an aliquot of the vaccine was thawed at room temperature and further diluted 1 in 10
85 using nuclease-free water. 40 µL of the diluted vaccine was added to each 40-mL sample. This
86 spike was added after pasteurization and cooling based on preliminary analysis during protocol
87 development that indicated reduced recovery of BCoV when it was added to the sample prior to
88 the pasteurization step. On the contrary, we found pasteurization to increase the measured
89 concentration of the N1 target in our samples, as compared to samples analyzed without the
90 initial pasteurization step (data not shown).

91

92 Solids were then removed from samples through centrifugation at 5000 x g for 10 min at 4 °C
93 (Eppendorf Centrifuge 5804 R or Thermo Fisher Scientific Sorvall X4 Pro Centrifuge). Sample
94 supernatant was filtered using 0.22 µm cellulose acetate filters (Corning, 431154). It should be
95 noted that due to brief challenges in obtaining some consumables during the fall of 2020 due to
96 supply chain constraints, alternative filters were used for some batches of samples—namely, (1)
97 0.45 µm cellulose nitrate filters (Thermo Scientific Nalgene, 130-4045PK) for samples collected
98 on October 4, 6, and 18, 2020 and (2) 0.22 µm polyethersulfone (Millex-GP, SLGP033RS) for
99 samples collected on November 1, 3, 8, and 10, 2020. A preliminary study indicated that filter
100 type and size may impact virus recovery, so if filters must be used, consistency of filter type and
101 size is preferable.

102

103 The utility of including the filtration step for sample processing and SARS-CoV-2 virus
104 extraction depends on downstream analysis goals. For example, if extracted RNA will be used
105 for sequencing applications, sample filtration can aid in removing bacterial cells and their nucleic
106 acids, thereby helping to enrich for viral RNA. Preliminary work during protocol development
107 indicated no significant difference between SARS-CoV-2 N1 gene copy concentrations in
108 samples analyzed with and without filtration with 0.22 µm cellulose acetate filters (data not
109 shown). Nonetheless, despite similar viral recoveries with and without filtration, we chose to
110 include the filtration step given logistical benefits, including the prevention of clogging of
111 membranes used in spin-column based RNA extraction methods, and ensuring that no solids
112 were carried over after the centrifugation step. Avoiding the transfer of solids could potentially
113 reduce variability caused by the inclusion of viruses associated with solid material, although
114 further analysis is needed to better understand the distribution of the virus in liquid and solid
115 fractions of wastewater samples and the impact of pasteurization on virus partitioning between
116 these two phases.

117

118 To concentrate viruses in solution, filtered samples were added to 4.0 g of PEG (Fisher
119 Scientific, BP233) and 0.9 g of NaCl (Fisher Scientific, BP358) in 50-mL Oak Ridge high-speed
120 polypropylene copolymer centrifuge tubes (Thermo Scientific Nalgene, 3119-0050), shaken by
121 hand until translucent, and held at 4 °C overnight. Note that 50-mL Oak Ridge high-speed
122 polycarbonate centrifuge tubes (Thermo Scientific Nalgene, 3138-0050) were initially used for
123 sample processing; however, these tubes broke after several uses, possibly due to the
124 polycarbonate's limited resistance to chemicals used in the RNA extraction (see below). The
125 next day, samples were centrifuged at 12,000 x g for 120 min at 4 °C (Eppendorf Centrifuge
126 5804 R or Thermo Fisher Scientific Sorvall X4 Pro Centrifuge) to pellet the PEG and associated
127 virus particles.

128

129 RNA was extracted from concentrated PEG pellets using the Qiagen QIAamp Viral RNA Mini
130 Kit (Qiagen, 52906; ethanol purchased separately, Fisher Scientific, BP2818500) following the
131 vacuum protocol with a QIAvac 24 Plus (Qiagen, 19413), with the modifications specified here.
132 First, 1.6x the suggested lysis buffer volume (i.e., 1.7 mL) was added directly to the PEG pellet
133 in the Oak Ridge polycarbonate tube in which it was centrifuged to ensure recovery of the entire

134 pellet. Note that samples processed prior to February 1, 2021 were extracted with 3x the
135 suggested lysis buffer volume, originally used in an effort to maximize PEG pellet recovery. A
136 subsequent study confirmed no significant difference in recovery using either 1.6x or 3x the
137 suggested lysis buffer volume (data not shown). RNA was eluted in 60 μ L of kit-supplied AVE
138 buffer through a series of two 30 μ L-elutions (Eppendorf Centrifuge 5424 R) and stored in
139 aliquots at -80 $^{\circ}$ C until quantification by RT-qPCR.

140

141 **RT-qPCR Assays**

142 ***SARS-CoV-2 N1 Assay***

143 A one-step RT-qPCR assay based on the CDC Diagnostic Panel was used to quantify gene
144 copies of the N1 region of the SARS-CoV-2 (GenBank accession no. MN908947) nucleocapsid
145 (N) gene [72-base amplicon, 28287 (starting position) - 28358 (ending position)].³⁻⁵ Triplicate 20
146 μ L reactions each contained 5 μ L of 4x TaqPath 1-Step RT-qPCR Master Mix (Thermo Fisher
147 Scientific, A15299); 1.5 μ L of the 2019-nCoV RUO Kit primer/probe mix (Integrated DNA
148 Technologies, 10006713) containing 6.7 μ M forward primer (5'-
149 GACCCCAAATCAGCGAAAT-3'), 6.7 μ M reverse primer (5'-
150 TCTGGTTACTGCCAGTTGAATCTG-3'), and 1.7 μ M probe (5'-FAM-
151 ACCCCGCATTACGTTTGGTGGACC-BHQ-1-3'); 5 μ L of template RNA; and 8.5 μ L of
152 nuclease-free water. Note that initial 2019-nCoV RUO Kits contained probes synthesized with
153 Black Hole Quencher 1 (BHQ-1), while later kits contained probes synthesized with
154 Zen/IowaBlack quenchers, according to correspondence with Integrated DNA Technologies.
155 Thus, RT-qPCR conducted later in the study period used probes with Zen/IowaBlack quenchers.
156 Data provided by the CDC for the limit of detection equivalence between probes with the two
157 quencher types showed that the lowest detectable concentration at which all replicates were
158 positive was the same for the two quencher types when using TaqPath 1-Step RT-qPCR Master
159 Mix.⁴

160

161 Each 96-well RT-qPCR plate included triplicate no template controls (nuclease-free water).
162 Synthetic SARS-CoV-2 RNA covering > 99.9% of the viral genome (Twist Bioscience Control
163 1, GENBANK ID MT007544.1; Twist Bioscience, 102019) served as both a positive control and

164 standard used in a decimal serial dilution for quantification of N1 gene copies. Standard
165 concentrations used for quantification ranged from 5×10^5 copies/rxn (equivalent to 1.5×10^8
166 copies/L of sample) to the limit of quantification (LOQ), which was 50 copies/rxn (equivalent to
167 1.5×10^4 copies/L of sample). The LOQ, determined as described by Forootan et al. 2017,⁶ was
168 the concentration for which the coefficient of variation (CV) on concentrations of replicate
169 standards calculated using measured C_q values was $\leq 35\%$ (CV = 34% for the LOQ in this
170 study). Note that these concentrations are relative to the approximate concentration of synthetic
171 RNA control reported by the manufacturer, as described in the main text.

172

173 Reactions were aliquoted manually into 0.1 mL MicroAmp™ Fast Optical 96-Well Reaction
174 Plates (Thermo Fisher Scientific, 4346907), which were covered with MicroAmp™ Optical
175 Adhesive Films (Thermo Fisher Scientific, 4311971). RT-qPCR analysis for the SARS-CoV-2
176 N1 gene was conducted on a StepOnePlus Real-Time PCR System (ThermoFisher, 4376600)
177 with the following cycling conditions: hold at 25 °C for 2 min, 50 °C for 15 min, and 95 °C for 2
178 min, followed by 45 cycles of 95 °C for 3 sec and 55 °C for 30 sec. The MIQE checklist for
179 reporting essential and desirable information⁷ for the N1 assay can be found in Table S.2.

180

181 **Table S.2. MIQE checklist: Essential and desirable information for the SARS-CoV-2 N1**
 182 **target RT-qPCR assay⁷**

ITEM TO CHECK	IMPORTANCE	CHECKLIST
EXPERIMENTAL DESIGN		
Definition of experimental and control groups	E	Provided in Materials and Methods
Number within each group	E	Provided in Materials and Methods
Assay carried out by core lab or investigator's lab?	D	Assay carried out by NYC DEP lab
Acknowledgement of authors' contributions	D	--
SAMPLE		
Description	E	Provided in Materials and Methods
Volume/mass of sample processed	D	Provided in Materials and Methods
Microdissection or macrodissection	E	N/A
Processing procedure	E	Provided in Materials and Methods
If frozen - how and how quickly?	E	N/A
If fixed - with what, how quickly?	E	N/A
Sample storage conditions and duration (especially for FFPE samples)	E	Provided in Materials and Methods
NUCLEIC ACID EXTRACTION		
Procedure and/or instrumentation	E	Provided in Materials and Methods /SI
Name of kit and details of any modifications	E	Provided in Materials and Methods /SI
Source of additional reagents used	D	Provided in SI
Details of DNase or RNase treatment	E	N/A
Contamination assessment (DNA or RNA)	E	Method blanks included
Nucleic acid quantification	E	RNA concentrations not routinely measured
Instrument and method	E	N/A
Purity (A260/A280)	D	N/A
Yield	D	N/A
RNA integrity method/instrument	E	Not determined
RIN/RQI or Cq of 3' and 5' transcripts	E	N/A
Electrophoresis traces	D	N/A
Inhibition testing (Cq dilutions, spike or other)	E	Discussed in Results and Discussion
REVERSE TRANSCRIPTION		
Complete reaction conditions	E	Provided in SI
Amount of RNA and reaction volume	E	Provided in SI
Priming oligonucleotide (if using GSP) and concentration	E	Provided in SI
Reverse transcriptase and concentration	E	Provided in SI
Temperature and time	E	Provided in SI

Table S.2. MIQE checklist *continued*

Manufacturer of reagents and catalogue numbers	D	Provided in SI
Cqs with and without RT	D*	Not determined
Storage conditions of cDNA	D	N/A (one-step RT-qPCR)
qPCR TARGET INFORMATION		
If multiplex, efficiency and LOD of each assay.	E	N/A
Sequence accession number	E	Provided in SI
Location of amplicon	D	Provided in SI
Amplicon length	E	Provided in SI
<i>In silico</i> specificity screen (BLAST, etc)	E	N/A
Pseudogenes, retropseudogenes or other homologs?	D	N/A
Sequence alignment	D	N/A
Secondary structure analysis of amplicon	D	N/A
Location of each primer by exon or intron (if applicable)	E	N/A
What splice variants are targeted?	E	N/A
qPCR OLIGONUCLEOTIDES		
Primer sequences	E	Provided in SI
RTPrimerDB Identification Number	D	Not provided
Probe sequences	D**	Provided in SI
Location and identity of any modifications	E	N/A
Manufacturer of oligonucleotides	D	Provided in SI
Purification method	D	Not provided
qPCR PROTOCOL		
Complete reaction conditions	E	Provided in SI
Reaction volume and amount of cDNA/DNA	E	Provided SI (one-step RT-qPCR)
Primer, (probe), Mg ⁺⁺ and dNTP concentrations	E	Provided in SI (TaqPath™ 1-Step RT-qPCR Master Mix, CG)
Polymerase identity and concentration	E	Provided in SI (TaqPath™ 1-Step RT-qPCR Master Mix, CG)
Buffer/kit identity and manufacturer	E	Provided in SI (TaqPath™ 1-Step RT-qPCR Master Mix, CG)
Exact chemical constitution of the buffer	D	Provided in SI (TaqPath™ 1-Step RT-qPCR Master Mix, CG)
Additives (SYBR Green I, DMSO, etc.)	E	N/A
Manufacturer of plates/tubes and catalog number	D	Provided in SI
Complete thermocycling parameters	E	Provided in SI
Reaction setup (manual/robotic)	D	Provided in SI
Manufacturer of qPCR instrument	E	Provided in SI

Table S.2. MIQE checklist *continued*

qPCR VALIDATION		
Evidence of optimisation (from gradients)	D	Not determined
Specificity (gel, sequence, melt, or digest)	E	N/A
For SYBR Green I, Cq of the NTC	E	N/A
Standard curves with slope and y-intercept	E	Provided in SI
PCR efficiency calculated from slope	E	Provided in SI
Confidence interval for PCR efficiency or standard error	D	Provided in SI
r ² of standard curve	E	Provided in SI
Linear dynamic range	E	Provided in SI
Cq variation at lower limit	E	Provided in SI
Confidence intervals throughout range	D	Not provided
Evidence for limit of detection	E	Provided in Materials and Methods
If multiplex, efficiency and LOD of each assay.	E	N/A
DATA ANALYSIS		
qPCR analysis program (source, version)	E	Provided in SI
Cq method determination	E	Provided in SI
Outlier identification and disposition	E	Provided in SI
Results of NTCs	E	Provided in Materials and Methods
Justification of number and choice of reference genes	E	N/A
Description of normalisation method	E	N/A
Number and concordance of biological replicates	D	N/A
Number and stage (RT or qPCR) of technical replicates	E	Provided in Materials and Methods
Repeatability (intra-assay variation)	E	Triplicate RT-qPCR reactions (SD included)
Reproducibility (inter-assay variation, %CV)	D	Not determined
Power analysis	D	Not determined
Statistical methods for result significance	E	N/A
Software (source, version)	E	Provided in SI
Cq or raw data submission using RDML	D	Not provided

183

184

185

186 Cq values were determined based on the automatic Cq threshold assigned by the StepOne™
187 Software v2.3 (ThermoFisher). The mean and standard deviation of automatic Cq threshold
188 across all plates were 0.30 and 0.065, respectively. Any RT-qPCR plates assigned an automatic
189 Cq threshold more than two standard deviations above or below the mean automatic Cq
190 threshold were designated as outlier Cq thresholds and reanalyzed with a manual Cq threshold
191 set at 0.31, the mean Cq threshold calculated after the outlier Cq thresholds were removed.

192

193 An approximate concentration of the synthetic RNA control used for standard curve preparation
194 was specified by the supplier. Concentrations of standards prepared from the first lot of this
195 control purchased by the research team (referred to as the “original” lot) were determined
196 assuming this approximate concentration. Data from nine standard curves generated with the
197 original lot of synthetic RNA control (analyzed on different RT-qPCR plated on different days)
198 were pooled to obtain one reference standard curve for the original lot. RNA target
199 concentrations of subsequent lots of the synthetic RNA control were each different from that of
200 the original lot, as evidenced by different Cq values of each point on the standard curve (data not
201 shown). Because absolute quantification (e.g., using ddPCR) of the RNA control was not
202 feasible at the time that sample analysis began, concentrations of subsequent lots of the RNA
203 control were quantified using measured Cq values of the new lot of the RNA control and the
204 pooled reference standard curve for the original lot (i.e., assuming the approximate quantity
205 reported by the manufacturer). Note that quantification of the RNA control through digital PCR
206 is underway, and N1 concentrations reported in the current version of this work may therefore be
207 updated in future versions to reflect the quantified concentration of the RT-qPCR standard.

208

209 The quality assurance and quality control guidelines developed internally for the NYC DEP’s
210 SARS-CoV-2 monitoring program established an acceptable range of amplification efficiencies
211 between 70% and 115%. PCR amplification efficiencies for all N1 assay plates ranged between
212 72% and 109%, with R^2 values for all standard curves ≥ 0.97 . Of the 37 individual N1 assay
213 plates from the study period (samples collected between November 8, 2020 and April 11, 2021),
214 two resulted in efficiencies less than 85% and none resulted in an efficiency over 110%,
215 indicating consistent acceptable performance of the assay over the five-month period of
216 statistical analysis. It should be noted that variations in amplification efficiency--calculated based

217 on the slope of the standard curve--may reflect errors or inconsistencies in preparation of
218 standards rather than changes in actual PCR amplification efficiency of the assay. We considered
219 variation in standard preparation a possibility, given that RT-qPCR plates were prepared by
220 multiple analysts, with new serial dilutions of the standard prepared for each plate. To account
221 for this potential variability and reduce any resulting noise in the data, we elected to apply a
222 pooled standard curve to calculate N1 concentrations of all samples. The pooled standard curve
223 was developed by combining data of standard curves from 56 plates (samples from September 8,
224 2020 to April 11, 2021); standard curves were pooled after the concentration adjustments of each
225 lot of the RNA control described above were performed. The resulting pooled standard curve had
226 a slope = -3.52, PCR efficiency = 92% (with 95% confidence interval of 91% to 94%), y-
227 intercept = 41.01, and $R^2 = 0.99$. A comparison of N1 concentrations measured for the Wards
228 Island facility using (a) individual and (b) pooled standard curves (Figure S.1) demonstrates how
229 this approach addresses variability due to errors during standard curve preparation without
230 affecting general trends in the data.

231

232

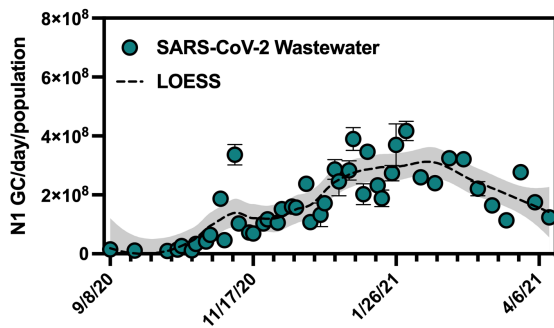
233

234

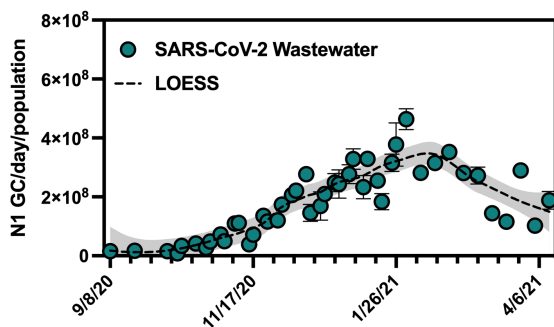
235

236

a. Individual RT-qPCR Standard Curves



b. Pooled RT-qPCR Standard Curve



237

238 **Figure S.1. SARS-CoV-2 viral loads in wastewater from the Wards Island facility**
239 **calculated using (a) the individual standard curves associated with the RT-qPCR plate on**
240 **which each sample was run and (b) the pooled standard curve.**

241 Influent SARS-CoV-2 viral loads were normalized by the sewershed population. Error bars
242 indicate standard deviations from triplicate RT-qPCR reactions as well as standard deviations of
243 duplicate samples, where applicable. The dashed black line represents a LOESS fit (span = 0.4),
244 with the 95% confidence intervals shaded in grey.

245
246

247 *B*CoV Assay

248 A one-step RT-qPCR assay adapted from previously published assays^{2,8,9} targeting the
249 transmembrane (M) gene of BCoV was used to assess recovery of the process control (primers
250 and probes purchased from Integrated DNA Technologies). Triplicate 20 μ L reactions each
251 contained 5 μ L of TaqPath 1-Step RT-qPCR Master Mix (4x, ThermoFisher), 1.5 μ L of the
252 primer/probe mix containing 5 μ M forward primer (5'- CTGGAAGTTGGTGGAGTT-3'), 5 μ M
253 reverse primer (5'- ATTATCGGCCTAACATACATC-3'), and 2.5 μ M probe (5'-FAM-
254 CCTTCATAT/Zen/CTATACACATCAAGTTGTT/3IABkFQ-3'), 5 μ L of template RNA, and
255 8.5 μ L of nuclease-free water. Each PCR plate included triplicate no template controls (nuclease-
256 free water). A custom gBlocks gene fragments oligo (Integrated DNA Technologies) (5'-

257 GTATCAGGTTGTTTATTAGAACTGGAAGTTGGTGGAGTTTCAACCCAGAAACAAACA
258 ACTTGATGTGTATAGATATGAAGGGAAGGATGTATGTTAGGCCGATAATTGAGGAC
259 TACCATACCCTTA-3') served as both the positive control and standard used in a decimal serial
260 dilution for quantification of gene copies. RT-qPCR analysis was conducted on a StepOnePlus
261 Real-Time PCR System (ThermoFisher) with the following cycling conditions: hold at 25 °C for
262 2 min, 50 °C for 15 min, and 95 °C for 12 min, followed by 45 cycles of 95 °C for 3 sec, 55 °C
263 for 30 sec, and 60 °C for 1 min.

264

265 Relative standard deviations (*RSD*) of both N1 concentrations and BCoV target concentrations
266 for duplicate samples were calculated using equation S1, where SD_{GC} is the standard deviation
267 and AVG_{GC} is the average gene copy concentration from duplicate samples, each with triplicate
268 RT-qPCR reactions.

$$269 \quad RSD = \frac{SD_{GC}}{AVG_{GC}} \times 100\% \quad \text{Equation S1}$$

270 In general, the relative standard deviation for concentrations of the BCoV target were not
271 consistent with those of the N1 target in a given sample, indicating that quantified recovery of
272 the BCoV control inoculated into samples before virus concentrations and extraction may not
273 accurately reflect recovery of SARS-CoV-2. Limitations of using proxy control viruses have
274 been discussed elsewhere.¹⁰ Calculated recoveries based on the known concentration of the
275 BCoV control spike were therefore not used to adjust N1 gene copy concentrations. However, if
276 the BCoV control was not recovered in any sample for which N1 was also not detected, that
277 sample was flagged for failed processing and was excluded from trend analysis or, when
278 possible, full analysis starting from pasteurization was repeated. If the BCoV control was
279 detected in a sample, any non-detect wells from the N1 target assay for that sample were
280 assigned a concentration of zero, which was used in calculating the reported average
281 concentration from triplicate wells.

282

283 **Publicly Available Clinical COVID-19 Data and Hospitalization Data**

284

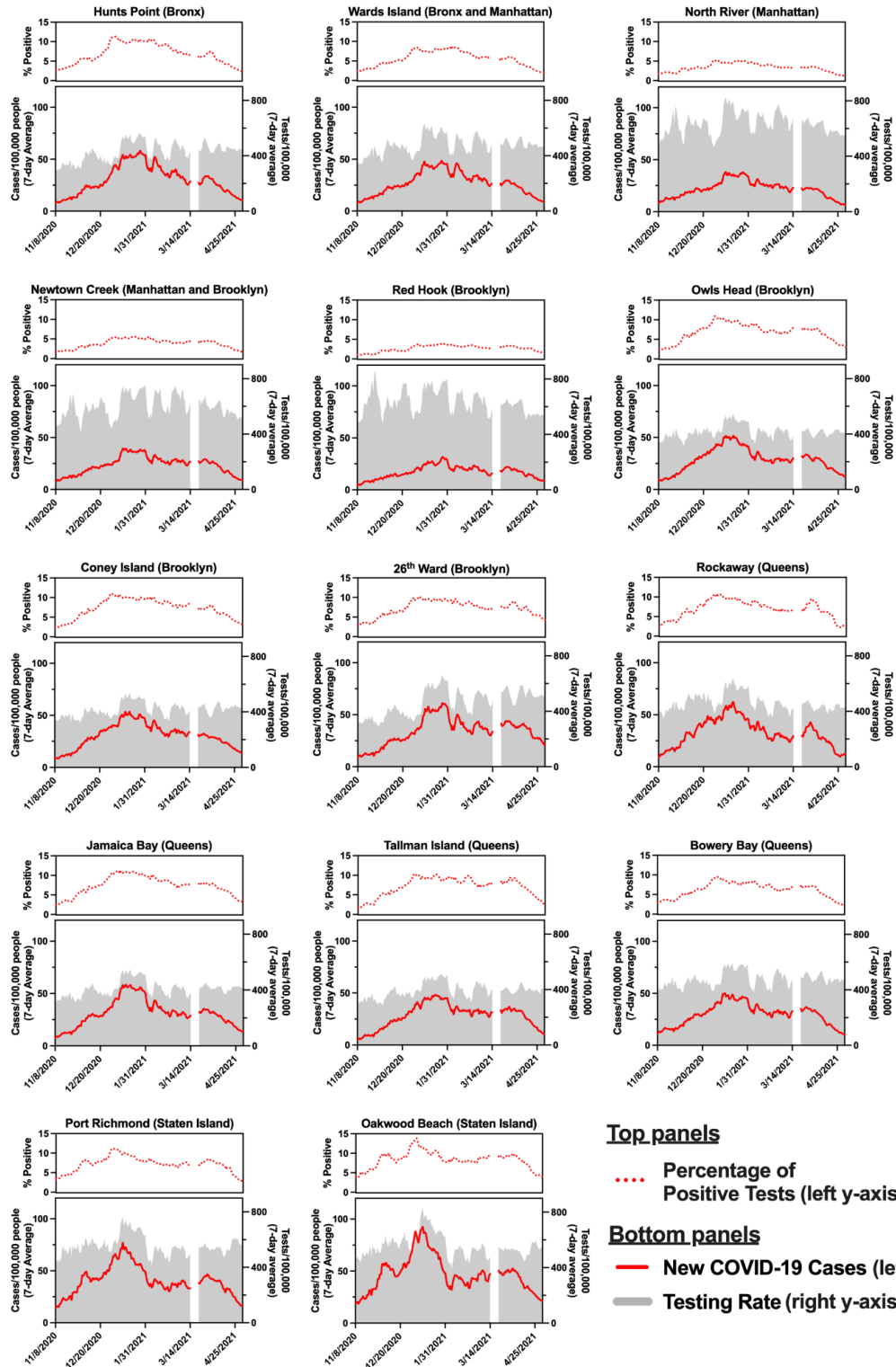
285 Figure S.2. summarizes the COVID-19 clinical testing data set obtained from publicly available
286 data provided by the NYC Department of Health and Mental Hygiene (DOHMH). Figure S.2.
287 includes, for each sewershed, the 7-day average of (1) the percentage of positive clinical
288 COVID-19 tests, (2) new cases/day, and (3) tests/day for the past 7 days. Note that the
289 percentage of positive clinical COVID-19 tests calculated as described in the main text, using the
290 “last7days-by-modzcta.csv” data set, differs from the percent positivity calculated by NYC
291 DOHMH in publicly available data sets such as “percentpositive-by-modzcta.csv”, which
292 accounts for duplication related to an individual being tested more than once during a 7-day
293 period.¹¹ The percentage of positive clinical COVID-19 tests we calculated for this analysis was
294 used only for an estimate of adequate testing (i.e., for filtering the combined data set to remove
295 data for dates with percentages of positive molecular tests (7-day average) that exceeded 10%)
296 and not for direct comparison to the wastewater data. Data from March 15, 2021 - March 21,
297 2021 were omitted due to technical issues related to data transmission. COVID-19 case data used
298 in correlation and linear regression analyses were not normalized by population.

299

300 Figure S.3 summarizes borough-level hospitalizations from the NYC DOHMH’s publicly
301 available “hosp-by-day.csv” file.¹¹ Borough populations were based on MODZCTA-level
302 population estimates from the NYC DOHMH’s NYC Coronavirus Disease 2019 (COVID-19)
303 Data.¹¹ Detailed information for the publicly available datasets was retrieved from:

304 <https://github.com/nychealth/coronavirus-data>.

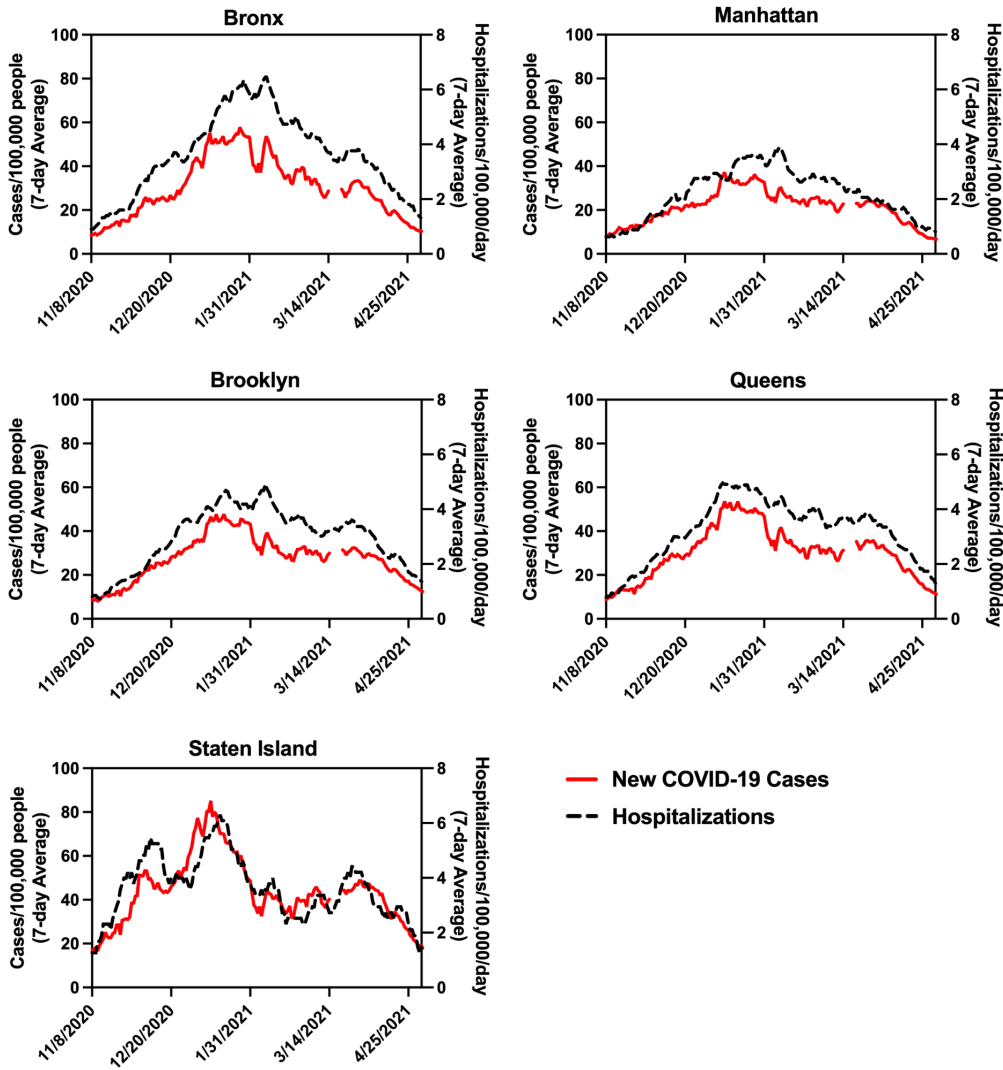
305



306
307
308
309

Figure S.2. Summary of COVID-19 testing data (molecular tests) for each sewershed in New York City.

310 Figure S.2. *caption continued from previous page.* For each sewershed, top panels: 7-day
 311 average of the percentage of positive clinical COVID-19 tests for the past 7 days. Bottom panels:
 312 7-day average of new cases/day for the past 7 days (left y-axes) and 7-day average of tests/day
 313 for the past 7 days (right y-axes), both normalized by the estimated sewershed population. Note
 314 that the left and right y-axes in the bottom panels have different scales. Data used for correlation
 315 analysis described in the main manuscript text is shown (November 8, 2020 to May 2, 2021).
 316
 317



318
 319 **Figure S.3. Summary of 7-day averages of new cases (solid red line) and hospitalizations**
 320 **(dashed black line) normalized by borough population for each New York City borough for**
 321 **the study period.**
 322 Data is organized by the last date in the 7-day period for which average was calculated. Note that
 323 the left and right y-axes have different scales.

324 **Sewershed-level Spearman’s Rank Correlation Coefficients**

325 **Table S.3. Spearman’s rank correlation coefficients (ρ) between SARS-CoV-2 wastewater**
 326 **data and clinical COVID-19 case data for each sewershed in New York City.**

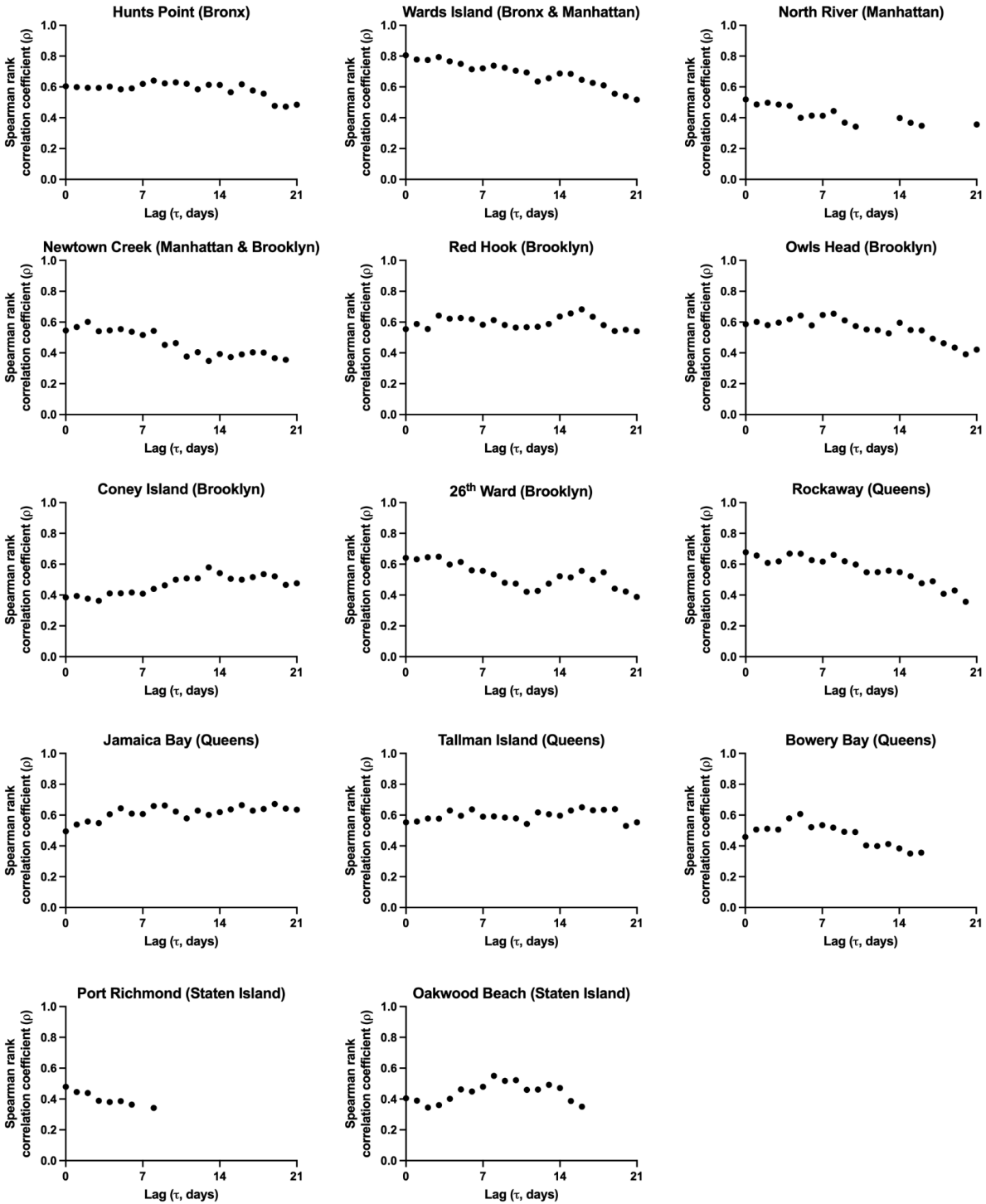
327 Column 1: Coefficients for correlations between SARS-CoV-2 *viral loads* in wastewater (N1
 328 GC/day) and 7-day averages of new COVID-19 cases/day, as described in the main manuscript
 329 text. Column 2: Coefficients for correlations between SARS-CoV-2 *concentrations* in
 330 wastewater (N1 GC/L) and 7-day averages of new COVID-19 cases/day normalized by
 331 sewershed populations. The alternative analysis presented in column 2 was used to assess any
 332 differences in correlation strengths due to flow normalization of wastewater data (i.e., to
 333 calculate viral loads, column 1). Significance levels: *p < 0.05, **p < 0.01, ***p < 0.001,
 334 ****p < 0.0001.
 335

	Column 1	Column 2
Data used for correlation analysis	SARS-CoV-2 Viral Loads (N1 GC/day)	SARS-CoV-2 Concentrations (N1 GC/L)
	New COVID-19 cases/day	New COVID-19 cases/day/100,000
Hunts Point	0.60***	0.54***
Wards Island	0.81****	0.80****
North River	0.52**	0.49**
Newtown Creek	0.55***	0.52**
Red Hook	0.55***	0.51**
Owls Head	0.59***	0.56***
Coney Island	0.38*	0.39*
26th Ward	0.64****	0.59***
Rockaway	0.68****	0.66****
Jamaica Bay	0.49**	0.54***
Tallman Island	0.55***	0.52**
Bowery Bay	0.46**	0.38*
Port Richmond	0.48**	0.38*
Oakwood Beach	0.40*	0.41*

336 **Time Lag Analysis**

337

338 To assess whether SARS-CoV-2 viral loads (N1 GC/day) measured in wastewater were a leading
339 indicator for 7-day averages of new COVID-19 cases/day, Spearman's rank correlation
340 coefficients between the two for lag times ranging from 0-21 days for each sewershed were
341 assessed (Figure S.4). The time lag represents the number of days the clinical data was shifted
342 back in time in relation to the date of wastewater sample collection. The optimal lag time (i.e.,
343 the number of days the clinical data lagged behind the wastewater data to result in the strongest
344 correlation) varied for each sewershed, with minimal improvement in correlations associated
345 with a lag time (Figure S.4). No significant correlations were found between the optimal lag time
346 and the average testing rate for the study period for any sewersheds.



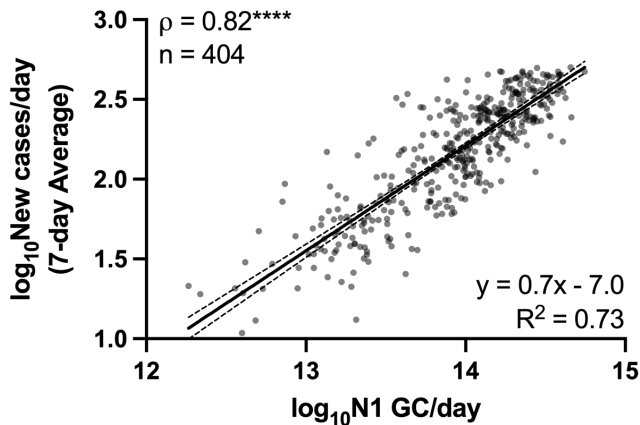
347

348 **Figure S.4. Spearman rank correlation coefficients (ρ) between SARS-CoV-2 viral loads**
 349 **(N1 GC/day) and 7-day averages of new COVID-19 cases/day, with a time lag (τ) between 0**
 350 **and 21 days for each sewershed in New York City.**

351 The time lag represents the number of days the clinical data was shifted back in time.
 352 Correlations that were not statistically significant ($p > 0.05$) have been omitted.

353 **Linear Regression Analysis**

354 Assessment of linear regressions presented in Figures 2 and 3 in the main manuscript confirmed
355 that (1) the slope between \log_{10} -transformed viral loads (N1 GC/day) and \log_{10} -transformed new
356 cases/day was significantly different from zero (F test; the assumption of significantly non-zero
357 slopes held true for both the combined data set and all facilities individually, with the exception
358 of Port Richmond), (2) a significant linear relationship was present (Pearson, $p < 0.05$; the
359 assumption of significant linear relationships held true for both the combined data set and all
360 facilities individually, with the exception of Port Richmond), (3) there were no clear patterns
361 observed in residuals (though exceptions were made for some outliers which we elected to retain
362 in the data), and (4) residuals were normally distributed based on the Shapiro-Wilks test ($\alpha =$
363 0.05) considered alongside visual inspection of histograms and quantile-quantile plots. Note that
364 linear regressions were performed using \log_{10} -transformed data; linear regressions with raw,
365 untransformed data generally resulted in fits with lower R^2 values and more frequent cases of
366 residuals that were not normally distributed than did regressions with the \log_{10} -transformed
367 transformed data set.



368

369 **Figure S.5. Linear regression of \log_{10} -transformed flow-normalized SARS-CoV-2 viral**
370 **loads in wastewater (N1 GC/day) and \log_{10} -transformed 7-day averages of new COVID-19**
371 **cases/day for the combined data set without the data filtered based on potentially**
372 **inadequate testing.**

373 This figure is presented for comparison to Figure 3 in the main text, which excludes data
374 collected on dates with over 10% positive testing results. The linear regression (solid line) and
375 associated 95% confidence intervals (dashed lines) are shown along with the goodness of fit R^2
376 value. The Spearman's rank correlation coefficient (ρ) between N1 GC/day and new COVID-19
377 cases/day is shown at the top left, with the significance level indicated ($****p < 0.0001$).

378 **Estimation of Minimum Detectable Case Rates**

379

380 Table S.4 summarizes the estimated minimum number of cases per day per 100,000 people in
381 each sewershed required to detect N1 in influent wastewater based on the method LOD.

382 Estimates were calculated using both individual linear regressions for each WRRF and the linear
383 regression for the combined data set using Equations 3 and 4 in the main text. To assess whether
384 the estimates calculated based on SARS-CoV-2 viral loads differed from those obtained using
385 SARS-CoV-2 concentrations without flow normalization, estimates were also determined using
386 linear regressions of N1 concentrations in wastewater (N1 GC/L) and new COVID-19
387 cases/day/100,000. The same range of estimates (2 - 8 cases/day/100,000) was obtained from
388 linear regressions using both pairs of data sets.

389

390 **Table S.4. Estimated minimum detectable case rates (new COVID-19 cases/day/100,000)**
 391 **associated with method LOD for quantification of the SARS-CoV-2 N1 gene target in**
 392 **wastewater (4,500 N1 GC/L) for each sewershed.**

393 The Oakwood Beach and Port Richmond sewersheds were excluded from analysis, as described in the main text, but
 394 information for all sewersheds is included here for completeness.

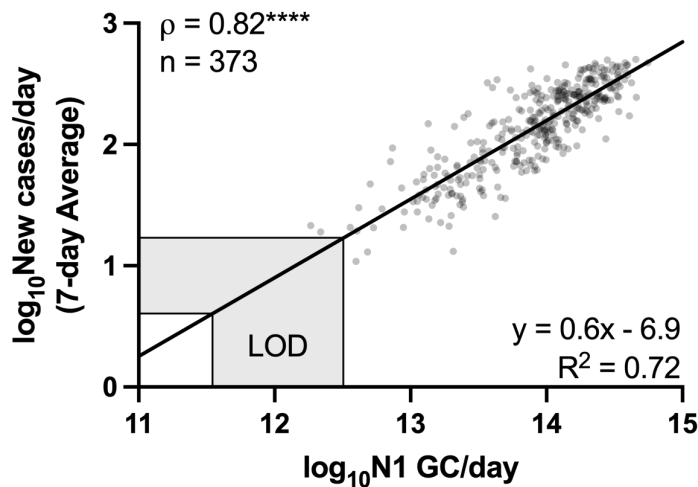
Sewershed (WRRF)	New COVID-19 cases/day/100,000 associated with method LOD					
	Based on linear regressions of N1 GC/day and new COVID-19 cases/day			Based on linear regressions of N1 GC/L and new COVID-19 cases/day/100,000 [†]		
	Sewershed-specific regressions	Regressions from combined data set*			Sewershed-specific regressions	Regression from combined data set
		(a) all data	(b) rise	(c) decline		
Hunts Point	5	2	2	3	5	5
Wards Island	2	2	2	2	2	
North River	8	2	2	2	8	
Newtown Creek	4	2	2	2	5	
Red Hook	3	2	2	3	4	
Owls Head	3	2	2	2	3	
Coney Island	6	2	2	2	6	
26th Ward	5	3	4	4	5	
Rockaway	8	4	4	5	8	
Jamaica Bay	2	2	2	2	3	
Tallman Island	2	3	3	3	3	
Bowery Bay	8	2	2	2	NA [‡]	
Port Richmond	NA [‡]	3	3	3	NA [‡]	
Oakwood Beach	20	3	3	3	21	

395 *Linear regressions were determined using (a) “all data”: all data from the combined data set, (b) “rise”: data from
 396 the combined data set associated with the rise in case rates (data prior to January 2021), or (c) “decline”: data from
 397 the combined data set associated with the decline in case rates (data after January 2021). Note that the combined
 398 data set does not include data from Port Richmond or Oakwood Beach and has been filtered to exclude data
 399 associated with over 10% positive tests.

400 [†]Estimates from these regressions are not flow-dependent; therefore, only one estimate is determined from the
 401 combined data set.

402 [‡]Slope of associated linear regression not significantly non-zero; linear regression rejected and case rate estimate not
 403 calculated

404 Figure S.6 illustrates graphically the approach used to estimate the equivalent number of
 405 COVID-19 cases/day/100,000 people associated with the SARS-CoV-2 quantification method
 406 LOD using linear regression for the combined data set. First, the method LOD was converted to
 407 a SARS-CoV-2 viral loading rate in wastewater (in units of N1 GC/day) for each sewershed
 408 using Equation 3 in the main text. The average daily flow rate for each WRRF (Q_{avg}) ranged
 409 from 21 MGD (Rockaway WRRF) to 188 MGD (Newtown Creek WRRF), resulting in a range
 410 of LOD-equivalent viral loads between 3.5×10^{11} to 3.2×10^{12} N1 GC/day across the facilities.
 411 The estimated minimum new COVID-19 cases/day required to detect SARS-CoV-2 in
 412 wastewater influent were determined by inputting this viral load into Equation 4 (main text) with
 413 the slope (m) and y-intercept (b) values from the linear regression (Figure S.6). The resulting
 414 COVID-19 cases/day (ranging from 4 to 17 new cases/day) were then normalized by the
 415 respective sewershed populations to obtain estimates ranging from 2 to 4 new COVID-19
 416 cases/day/100,000. The same approach was applied for each sewershed-level linear regression.
 417



418

419 **Figure S.6. Estimation of new COVID-19 cases/day associated with the method LOD for**
 420 **quantification of the SARS-CoV-2 N1 gene target in wastewater, based on the linear**
 421 **regression of \log_{10} -transformed SARS-CoV-2 viral loads (N1 GC/day) and \log_{10} -**
 422 **transformed 7-day averages of new COVID-19 cases/day for the combined data set**
 423 **(modified from Figure 3.a).**

424 The method LOD (in units of N1 GC/day) for the range of average flow rates (21 MGD at
 425 Rockaway WRRF - 188 MGD at Newtown Creek WRRF) for all facilities is indicated in the
 426 shaded grey region along the x-axis. The associated minimum detectable new COVID-19
 427 cases/day is indicated in the shaded grey region along the y-axis. Estimates from this approach
 428 were normalized by sewershed populations.

429 **References**

- 430 1 2050 SED Forecasts, <https://www.nymtc.org/DATA-AND-MODELING/SED->
431 Forecasts/2050-Forecasts, (accessed 12 April 2021).
- 432 2 S. Feng, A. Roguet, J. S. McClary-Gutierrez, R. J. Newton, N. Kloczko, J. G. Meiman and S.
433 L. McLellan, Evaluation of Sampling, Analysis, and Normalization Methods for SARS-CoV-
434 2 Concentrations in Wastewater to Assess COVID-19 Burdens in Wisconsin Communities,
435 *ACS EST Water*, 2021, **1**, 1955–1965.
- 436 3 X. Lu, L. Wang, S. K. Sakthivel, B. Whitaker, J. Murray, S. Kamili, B. Lynch, L. Malapati, S.
437 A. Burke, J. Harcourt, A. Tamin, N. J. Thornburg, J. M. Villanueva and S. Lindstrom, US
438 CDC Real-Time Reverse Transcription PCR Panel for Detection of Severe Acute Respiratory
439 Syndrome Coronavirus 2, *Emerg Infect Dis*, 2020, **26**, 1654–1665.
- 440 4 Centers for Disease Control and Prevention, Division of Viral Diseases, CDC 2019-Novel
441 Coronavirus (2019-nCoV) Real-Time RT-PCR Diagnostic Panel: Instructions for Use, CDC-
442 006-00019, Revision 06, 2020.
- 443 5 Division of Viral Diseases, National Center for Immunization and Respiratory Diseases,
444 Centers for Disease Control and Prevention, Atlanta, GA, USA, 2019-Novel Coronavirus
445 (2019-nCoV) Real-time rRT-PCR Panel Primers and Probes, 2020.
- 446 6 A. Forootan, R. Sjöback, J. Björkman, B. Sjögreen, L. Linz and M. Kubista, Methods to
447 determine limit of detection and limit of quantification in quantitative real-time PCR (qPCR),
448 *Biomol Detect Quantif*, 2017, **12**, 1–6.
- 449 7 S. A. Bustin, V. Benes, J. A. Garson, J. Hellemans, J. Huggett, M. Kubista, R. Mueller, T.
450 Nolan, M. W. Pfaffl, G. L. Shipley, J. Vandesompele and C. T. Wittwer, The MIQE
451 Guidelines: Minimum Information for Publication of Quantitative Real-Time PCR
452 Experiments, *Clin Chem*, 2009, **55**, 611–622.
- 453 8 N. Decaro, G. Elia, M. Campolo, C. Desario, V. Mari, A. Radogna, M. L. Colaianni, F.
454 Cirone, M. Tempesta and C. Buonavoglia, Detection of bovine coronavirus using a TaqMan-
455 based real-time RT-PCR assay, *J Virol Methods*, 2008, **151**, 167–171.
- 456 9 S. Loeb, One-Step RT-ddPCR for Detection of SARS-CoV-2, Bovine Coronavirus, and
457 PMMoV RNA in RNA Derived from Wastewater or Primary Settled Solids, *protocols.io*,
458 2020, DOI:10.17504/protocols.io.bi6vkhe6.
- 459 10 R. S. Kantor, K. L. Nelson, H. D. Greenwald and L. C. Kennedy, Challenges in Measuring the
460 Recovery of SARS-CoV-2 from Wastewater, *Environ. Sci. Technol.*, 2021, **55**, 3514–3519.
- 461 11 nychealth/coronavirus-data, <https://github.com/nychealth/coronavirus-data>, (accessed 20 May
462 2021).